

ENC-2022-0324

SEVERE SLUGGING IDENTIFICATION USING LONG-SHORT TERM MEMORY NETWORKS

C. M. Ruiz-Díaz

University of São Paulo (USP), São Carlos School of Engineering (ESSC), Mechanical Engineering Department, Industrial Multiphase Flow Laboratory (LEMI), Av. Trab. São Carlense, 400 - Parque Arnold Schimidt, São Carlos - SP, 13566-590, Brazil.

carlosruiz978@usp.br

Marlon M. Hernández-Cely

Federal University of Pelotas, Control and Automation Engineering, Engineering Center, Rua Benjamin Constant, n° 989, Porto, Pelotas - RS, 96010-020, Brazil.

marlon.cely@ufpel.edu.br

O. M. H. Rodriguez

University of São Paulo (USP), São Carlos School of Engineering (ESSC), Mechanical Engineering Department, Industrial Multiphase Flow Laboratory (LEMI), Av. Trab. São Carlense, 400 - Parque Arnold Schimidt, São Carlos - SP, 13566-590, Brazil.

oscarmhr@sc.usp.br

Abstract. *The production of oil and gas in offshore platforms involves a great number of potentially dangerous events of great complexity. Severe slugging is a flow anomaly that may result in flooding of production facilities and decrease in productivity, with characteristics of transient pressures, volumetric fractions, and superficial velocities. A study will be carried out in a vertical pipe with two-phase flow of liquid and gas, aiming to simulate severe slugging. Liquid injection will be carried out by means of a positive displacement pump with a frequency inverter, and dense gas is provided to the system by a booster specially designed to work with gas. The gas injection will be periodically modified by flow control valves installed upstream the test line. Directional control valves are installed in each injection line together with pressure, temperature and flow sensors, whose measurements are stored in a computerized control system, where the operation of all the experimental equipment is monitored and the data is saved. The information collected was optimized with data science techniques and used to develop a predictive model based on the technique of long- and short-term memory networks to predict the types of severe slugging inside pipelines. A correlation matrix was developed to determine the relationship of parameters in the formation of severe slugging, including the specific density of the gas-liquid mixture, gas-liquid ratio (GLR), superficial gas velocity, superficial liquid velocity, gas and liquid volumetric fractions. The parameters used to determine the performance of the AI model were the root mean square error (MSE), the Root Mean Square Error (RMSE) and the coefficient of determination (R^2), for which values of 0.33%, 5.7% and 0.9983 were obtained, respectively.*

Keywords: *severe slugging, long-short term memory networks, two-phase flow, dense gas*

1. INTRODUCTION

Multiphase flows are present in several industrial sectors around the world. Currently, the oil and gas industry has concentrated on minimizing the risks present in its production process, especially in the assurance of the flow generated in extreme conditions such as those present in offshore platforms, where the oil and gas mixture flows through pipes with different inclinations and exposed to different physical phenomena, such as temperature and pressure changes as the flow moves from the depths to the floating platforms.

Oil and gas mixtures are transported through flow lines with inclinations between 0° and 90° , whose geometries include a considerable variety of diameters and lengths. These parameters are determinant in the formation of flow patterns, since they are directly related to the superficial velocity of each fluid, gas fraction, liquid volumetric fraction, pressure variation in the transport line, among others.

Given the importance of knowing the flow behavior inside the pipes from physical and chemical parameters, analysis of the flow patterns generated in them is a fundamental concept, for this reason, these phenomena must be modeled with precision, to determine possible transitions that occur in processes with transient gas-liquid flows. Transition zones present between flow patterns developed in horizontal pipes with gas-liquid flow were studied by (Yehudah Taitel et al.,

1978), by implementing a methodology to predict them. An amplification and improvement of this methodology for flow pattern transition prediction was developed by (Yehuda Taitel et al., 1980), specifically for vertical pipelines with gas-liquid flow.

Flow pattern development in standpipes has also been studied by (Hasan & Kabir, 1986), where four general flow patterns are specified as bubbly, slug, churn and annular. Less desirable two-phase gas-liquid flow patterns are the intermittent ones, which are composed of bubbly and churns, especially severe slugging, studied for the first time by (Yocum, 1973) and investigations are still in progress, given the complexity of this phenomenon. Severe slugging is characterized by an elongated liquid slug, which generates fluctuations in the pressure levels inside the pipelines (Luo et al., 2014). Studies carried out by (Schmidt et al., 1980), determined that severe slugging only existed when there was a downward slope in the pipe upstream of the riser base.

To analyze this severe slugging phenomenon, a large amount of research both experimental and numerical such as those developed by (Baliño et al., 2010; Theyab & Theyab, 2018; Zhou et al., 2018), taking into account laboratory limitations, summarized in total pipe lengths of less than 56 [m], in conjunction with vertical risers with a maximum height of less than 20 [m]. To eliminate the structural limitations of the mentioned laboratories, solutions have been sought related to the implementation of artificial intelligence techniques that allow the development of predictive models that amplify the process simulation capacity, taking fluid parameters as inputs and generating as a result the identification of two-phase flow patterns (Goda et al., 2002; Ruiz-Diaz et al., 2022). Specifically (Wu et al., 2022) developed a model for the identification of different types of severe slugging generated in their experimental setup.

Artificial intelligence applied to multiphase flow is an innovated field that has been calling the attention of researchers over the last years in part due to the advancement of the autonomous processes for forecasting from experimental databases (Kagemoto, 2020). Different artificial intelligence techniques have been recently developed to predict flow regimes in horizontal pipelines (Alhashem, 2019; Mi et al., 2001; Quintino et al., 2020), based on the application of feed forward (FFNN) or recurrent neural networks (RNN), where the outputs of each predictive model are returned to the system together with new values of the inputs (Alkhalaf et al., 2019; Kagemoto, 2020). In this study, a long short term memory model that predicts the types of severe slugging under predefined experimental conditions was developed from the information collected by (Malekzadeh et al., 2012; Park et al., 2018) for two-phase gas-liquid flow.

2. METHODOLOGY

Two-phase gas-liquid flow experiments were carried out in structural assemblies consisting of 4 main sections: fluid supply, test zone (including horizontal, inclined downward and vertical upward sections), separation zone and control line. To analyze instabilities within the pipelines and describe the specific behaviors that developed when intermittent flow patterns were formed, (Park et al., 2018) and (Malekzadeh et al., 2012) structured closed pipe assemblies following the sections described above and developed their experiments at Korea Evaluation Institute of Industrial Technology (KEIT) and Shell Technology Center Amsterdam (STCA) respectively. The geometrical characteristics of such installations are presented in Table 1.

Table 1. Geometrical characteristics of experimental structures.

Author	Dataset	Section	Material	Geometry		
				Length [m]	I.D. [mm]	Inclination [°]
(Park et al., 2018)	I	Horizontal	Transparent PVC	14	50.8	0
		Declined	Transparent PVC	5.6		-15
		Vertical	Transparent PVC	6.5		90
(Malekzadeh et al., 2012)	II	Horizontal	Steel	65	50.8	0
		Declined	Perspex	35		-2.54
		Vertical	Transparent PVC	15.5	45	90

Parameters used to develop the intelligent model are presented in the following Table 2, including specific density of the gas-liquid mixture (ρ_s), gas-liquid ratio (GLR), superficial gas velocity (USG0), superficial liquid velocity (USL), gas volumetric fraction (α_G) and implicitly liquid volumetric fraction (α_L).

Table 2. Description of the dataset used for developing the LSTM model.

Dataset	Parameter	Value	Points	Flow pattern	
I	$\overline{\rho_s}$ [-]	0.23	56	SS1	15
	\overline{GLR} [-]	0.09		SS2	6

	USG0 [m/s]	0.8 - 2		SS3	17
	USL [m/s]	0.04 - 0.7		STB	12
	α_G [-]	0.5 - 0.97		USO	6
II	$\bar{\rho}_s$ [-]	0.14	46	SS1	10
	\overline{GLR} [-]	0.50		SS2	8
	USG0 [m/s]	0.34 - 4.11		SS3	11
	USL [m/s]	0.02 - 0.6		STB	8
	α_G [-]	0.45 - 0.98		USO	9

Specifically, ρ_s was determined for each combination of superficial velocities (US) and the respective volumetric fraction of the components of the biphasic mixture (ρ_G y ρ_L). This relation is mathematically modeled and presented in Eq. (1).

$$\rho_s = \frac{(\rho_G * \alpha_G) + (1 - \alpha_G) * \rho_L}{\rho_L} = \frac{(\rho_G * \alpha_G) + (\alpha_L * \rho_L)}{\rho_L} \quad (1)$$

According to study carried out by (Pots et al., 1987), GLR is a parameter of great influence in the formation of severe slugging, by making a comparison between the mass flow rate of gas (\dot{m}_G) and liquid (\dot{m}_L) flowing inside the pipe, assuming that there is no mass transfer between the phases, that $\rho_L \gg \rho_G$ and a vertical elevator is available. Equation (2) models mathematically this dimensionless ratio between mass flows, including the volumetric flow rate of gas \dot{Q}_G and liquid \dot{Q}_L , together with their respective densities.

$$GLR = \frac{\dot{m}_G}{\dot{m}_L} = \frac{\rho_G * \dot{Q}_G}{\rho_L * \dot{Q}_L} \quad (2)$$

Correlation matrix was structured to determine the correspondence between the parameters selected as inputs to the intelligent model, as shown in the following Figure 1, with values of proximity in the interval [-1, 1], with reflection on the main diagonal, identifying a great relationship between the parameters that, when making the vertical and horizontal superposition of their locations, give light and dark colors. Intermediate colors represent the relationship between one variable with the other is not very dependent, as is the case of specific density with diameter.

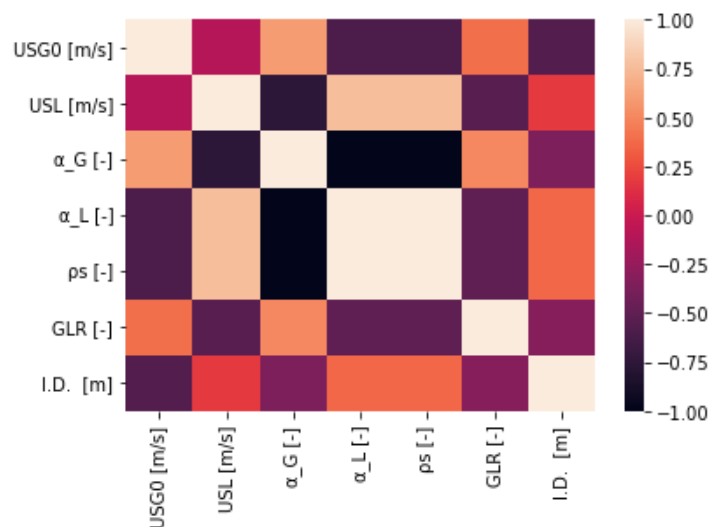


Figure 1. Correlation matrix.

Standardized information is presented in Figure 2, whose horizontal axis represents each of the variables indicated, and the vertical axis represents the amount of data with this normalized value. Additionally, a categorization function was applied to carry out the following distribution of levels for each type of severe slugging: SS1 (1.0), SS2 (2.0), SS3 (3.0), USO (4.0) and STB (5.0).

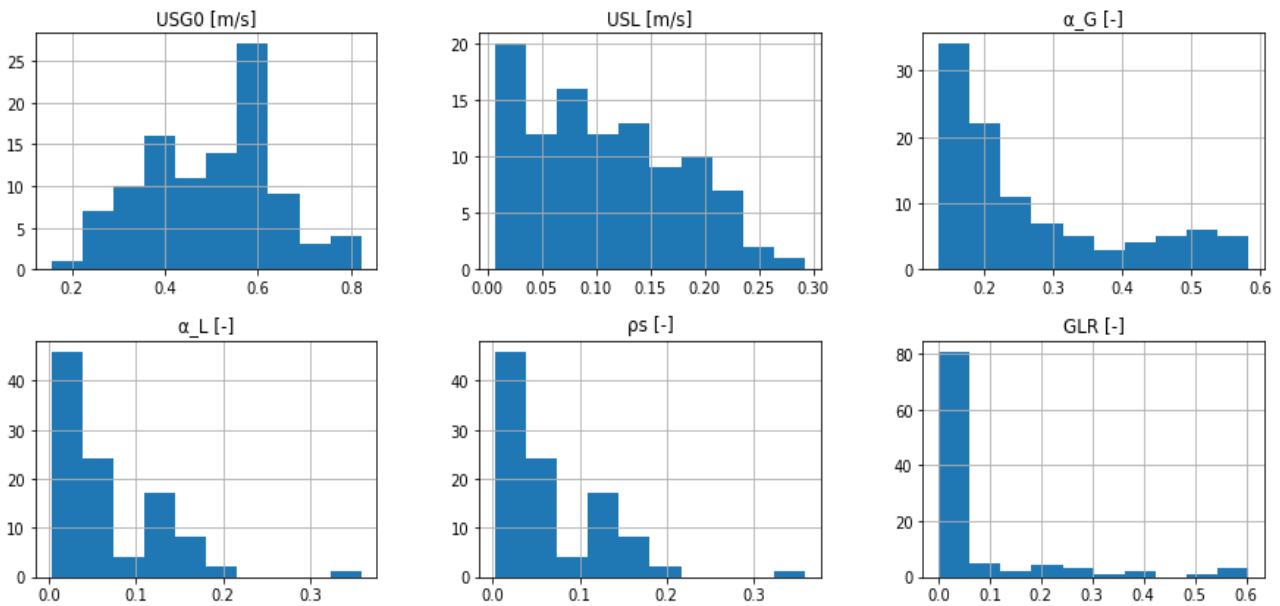


Figure 2. Standardized information.

3. SEVERE SLUGGING

Experimentally, five possible types of severe slugging were determined as shown in the flow pattern column of Table 2, based on stability characteristics of each flow regime and the transition between them. Classification developed was stable oscillation (STB), unstable oscillations (USO), severe slugging 1 (SS1), severe slugging 2 (SS2) and severe slugging 3 (SS3). Representative flow maps of datasets I and II are presented in Figure 3.

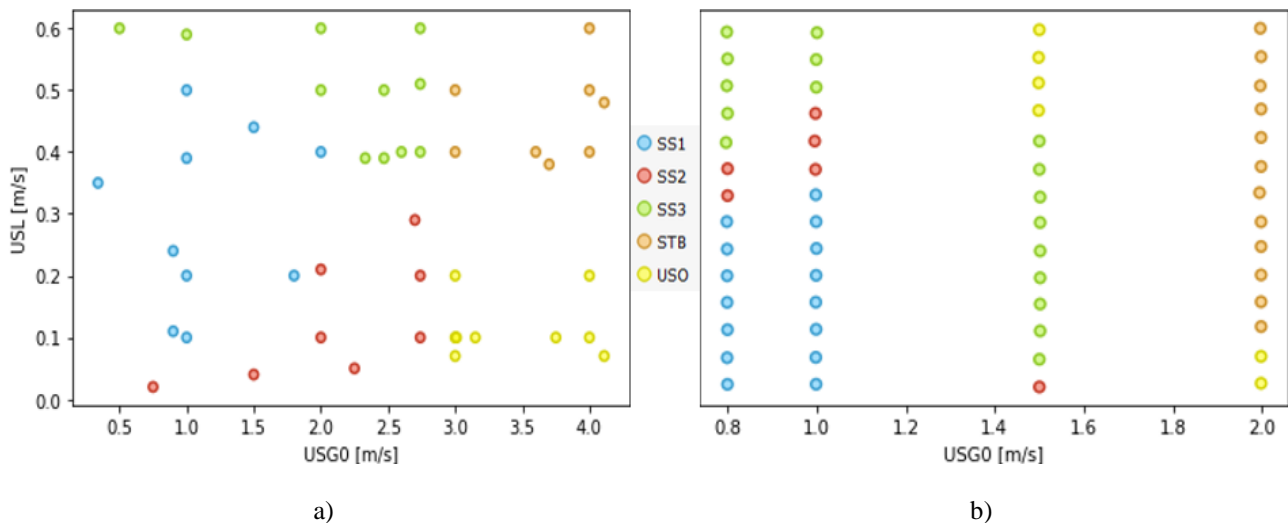


Figure 3. Flow pattern maps: a) from (Malekzadeh et al., 2012), b) from (Park et al., 2018).

Below are detailed the characteristics developed by each of the types of severe slugging identified:

3.1 Stable oscillations (STB)

This type of severe slugging occurs when working with high gas and liquid velocities inside the riser, presenting fluctuations in the pressure values inside the riser with an amplitude close to 40 [KPa] and with a high frequency for the two databases analyzed, i.e., the ΔP in the riser has a short period behavior.

3.2 Unstable oscillations (STB)

This flow pattern is characterized by ΔP values with a lower amplitude than the other types of severe slugging. Maximum experimental ΔP value reached by dataset II was 40 [KPa] starting its formation when USL and USG0 were 0.1 and 3.75 [m/s] respectively. Similarly, maximum experimental ΔP value reached by dataset I was 60 [KPa] when USG0 and USL were 1.5 and 0.5 [m/s] respectively.

3.3 Severe slugging 1 (SS1)

SS1 is generated for low USG0 with a gradual increase in USG0 and USL. Likewise, development of this flow pattern begins when the liquid starts to displace the gas column present in the riser and consecutively starts with the injection of gas that begins to displace the remaining water column of the previous sequence, thus generating the formation of elongated bubbles that increase their length as much water is injected, without exceeding the length of the liquid slug that in this case is greater or equal to the length of the riser eliminating the pressure drop due to friction. In this work, SS1 presents the particularity of reaching a maximum ΔP for dataset II of 153 [KPa], developing with USL of 0.2 [m/s] and USG0 of 1.0 [m/s] with a mean experimental period of 130 [s]. In dataset I, such flow pattern developed for USL of 0.05 [m/s] and USG0 of 0.8 [m/s].

3.4 Severe slugging 2 (SS2)

SS2 formation conditions are like those of SS1, only that for SS2 gas injection frequency is increased at the base of the vertical column length of the liquid slug, thus generating the liquid slug to be lower than height of the vertical riser. In this work, it was determined that SS2 formation is achieved upon reaching USL of 0.1 [m/s] and USG0 of 2.0 [m/s] along with a maximum ΔP of 125 [KPa] for dataset II and 30 [KPa] for dataset I upon reaching USL of 0.4 [m/s] and USG0 of 0.8 [m/s].

3.5 Severe slugging 3 (SS3)

SS3 begins its formation when the gas injection at the bottom of the riser begins to increase. Similarly, when USG0 begins to increase with USL not very low, the transition of SS1 and subsequent formation of SS3 begins when, despite increasing gas injection, liquid remains inside the riser. In this work a maximum ΔP of 60 [KPa] was determined for dataset I with USL of 0.5 [m/s] and USG0 of 0.8 [m/s]. For dataset II it was experimentally determined that SS3 was generated when USL of 0.39 [m/s] and USG0 of 2.33 [m/s] with a maximum ΔP of 152 [KPa].

4. DEVELOPMENT OF THE LSTM MODEL

The model to be developed will have in its internal structure a LSTM state cell which in general will have three main gates, one called input gate, which is responsible for feeding the intelligent system with new inputs and inputs from previous hidden cells or layers, the forget gate, which makes a detailed selection of the information to be memorized and the output gate, which stores the values generated by the predictive model. Schematically, Figure 4 presents the state cell to be implemented in our model, being X_t the input vector, $Y_{[t-1]}$ denotes the outputs generated by a previous cell or layer, $c_{[t-1]}$ denotes the information saved by a previous forget gate, $c_{[t]}$ denotes the output of the current forget gate and $Y_{[t]}$ denotes the output of the predictive model. The models in this study were developed considering Adam optimizer, different split ratios, LSTM layers, batch size and LSTM cells.

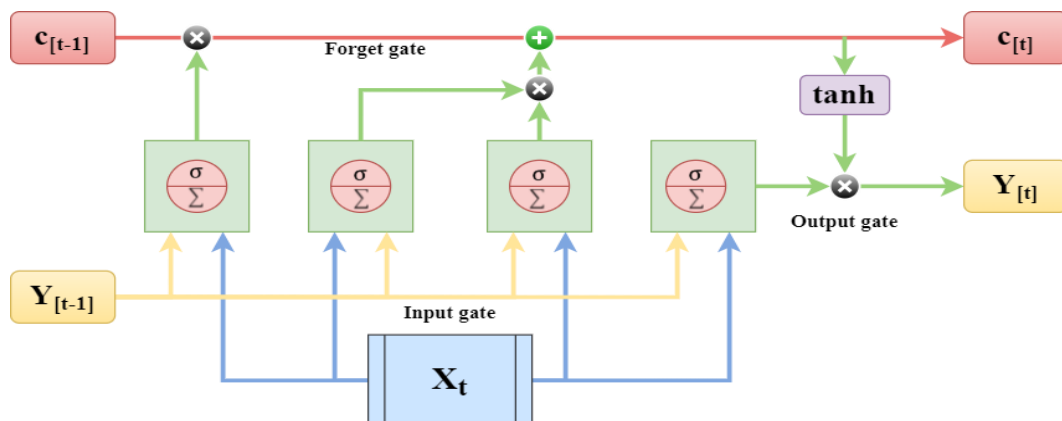


Figure 4. Long-short Term Memory structure.

4.1 Statistical parameters

Determination of the intelligent model with the best results, was given from the comparison between predictive values generated by each LSTM structuring and real values obtained experimentally from the literature. Statistical parameters selected are the mean squared error (MSE), root mean square error (RMSE), and correlation coefficient (R^2), defined in Equations (3), (4) and (5).

$$MSE = \frac{1}{n} \sum_{m=1}^n (Y_{(Exp,m)} - Y_{(Pred,m)})^2 \quad (3)$$

$$RMSE = \sqrt{\frac{\sum_{m=1}^n (Y_{(Exp,m)} - Y_{(Pred,m)})^2}{n}} \quad (4)$$

$$R^2 = 1 - \frac{\sum_{m=1}^n (Y_{(Exp,m)} - Y_{(Pred,m)})^2}{\sum_{m=1}^n (Y_{(Exp,m)} - \bar{Y}_{(Pred,m)})^2} \quad (5)$$

Where $Y_{(Exp)}$ represents the current value of the variable being calculated, $Y_{(Pred)}$ is the output of the predictive model, and $\bar{Y}_{(Pred,m)}$ is the average value of all the values generated by the intelligent system.

5. RESULTS AND DISCUSSION

Based on the simulations developed to obtain a predictive model that generally fits the information contained in each dataset, different network structures were developed, making use of LSTM cells, dense layers, an optimization metric called loss function and several epochs determined for each structure. Specific structuring of each model is presented in Table 3, which presents the Adam optimizer, a fixed number of epochs for all models (100), a range of batch sizes from 1 to 4 elements per set, the number of LSTM sows implemented and split ratios defined in two ways, corresponding to SR1 and SR2, directly related to the percentage of information that was used and in the validation of each model.

Table 3. Proposed models generalities.

Optimizer	Epochs	Batch size	LSTM cells	SR1	SR2
Adam	100	[1-4]	80	70% (train)	80% (train)
			100	30% (test)	20% (test)

Evaluation of developed models was carried out with application of defined statistical parameters (MSE, RMSE and R^2). Table 4 and Table 5 contain the results obtained for each model structuring, which was developed horizontally, defining the SR used, number of layers with LSTM, batch size and number of LSTM cells implemented. The value of each statistical parameter obtained for the developed combinations of hyperparameters is also presented.

Table 4. SR1 implementation results.

Split Ratio	LSTM layers	Batch size	LSTM cells	MSE	RMSE	R^2
SR1	1	1	80	0,3400	0,5831	0,8310
			100	0,3395	0,5826	0,8313
		2	80	0,3635	0,6029	0,8194
			100	0,3172	0,5632	0,8424
		3	80	0,2301	0,4797	0,8857
			100	0,2861	0,5349	0,8578
		4	80	0,1655	0,4068	0,9178
			100	0,2381	0,4880	0,8817
	2	1	80	0,0107	0,1033	0,9947
			100	0,0100	0,0998	0,9951
		2	80	0,0100	0,0998	0,9951
			100	0,0085	0,0923	0,9958
		3	80	0,0088	0,0937	0,9956
			100	0,0041	0,0638	0,9980
		4	80	0,0039	0,0625	0,9981

			100	0,0037	0,0605	0,9982
--	--	--	-----	--------	--------	--------

Table 5. SR2 implementation.

Split Ratio	LSTM layers	Batch size	LSTM cells	MSE	RMSE	R ²
SR2	1	1	80	0,2860	0,5348	0,8523
			100	0,3241	0,5693	0,8326
		2	80	0,2636	0,5134	0,8639
			100	0,2844	0,5333	0,8531
		3	80	0,2841	0,5330	0,8533
			100	0,2813	0,5304	0,8547
		4	80	0,2813	0,5304	0,8405
			100	0,2983	0,5461	0,8460
	2	1	80	0,0244	0,1562	0,9874
			100	0,0033	0,0574	0,9983
		2	80	0,0059	0,0765	0,9970
			100	0,0071	0,0844	0,9963
		3	80	0,2841	0,5330	0,8533
			100	0,0090	0,0951	0,9953
		4	80	0,0488	0,2210	0,9748
			100	0,0227	0,1506	0,9883

All 16 models developed with SR1 present MSE values below 40%, since the maximum MSE obtained is 36% when the developed configuration includes SR1, batch size of 2 and 80 cells in the only LSTM layer implemented. Similarly, the highest value for RMSE is presented for same structure, with a value close to 60%. This structure allows us to establish that, in this case, approximation levels between the experimental values and those obtained by the predictive model differ on a scale considered to reject the structure immediately.

In the 16 models developed with SR2, MSE values below 32%, since this was the maximum value presented, together with an RMSE of 56.9%, when implementing SR2, batch size of 1 and 100 cells in the single LSTM layer. Such structuring is also rejected.

Results obtained for the combination between each SR together with the respective LSTM layers, batch sizes and LSTM cells are presented in Figure 6, whose vertical axis represents the values between 0 and 1 for the parameters determined as MSE and R².

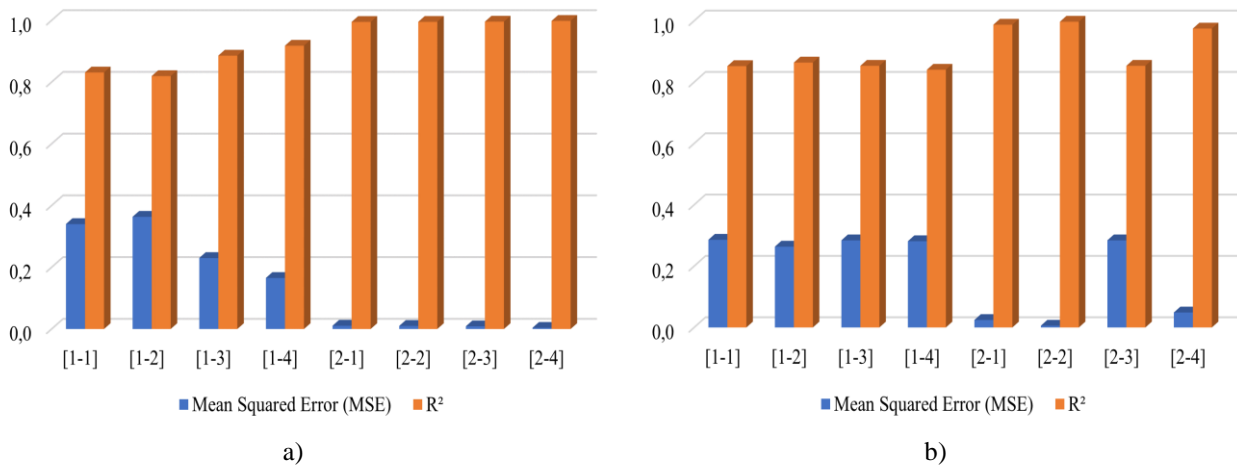


Figure 5. MSE and R² results with 80 LSTM cells, applying: a) SR1 and b) SR2.

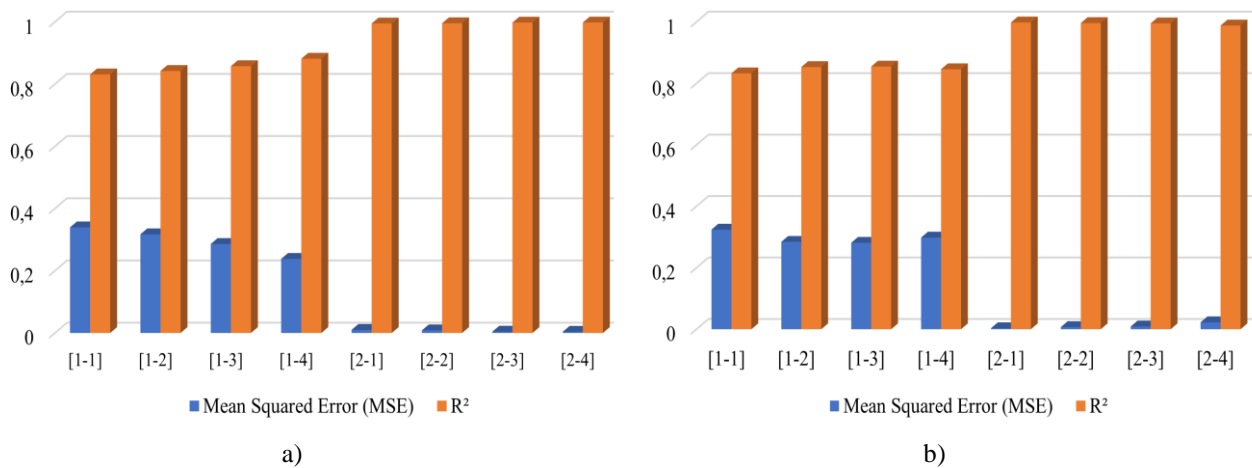


Figure 6. MSE and R² results with 100 LSTM cells, applying: a) SR1 and b) SR2.

Considering the bar diagrams schematized in Figure 5 and Figure 6, a stabilization of the R² with values close to 1 is detailed for structures [2-1], [2-2], [2-3], [2-4] and later, which indicates that the behavior followed by the predictive values together with the experimental ones is linear. The maximum R² value reached was 0.9983 together with an MSE of 0.33 % and MRSE of 0.0574, achieved by applying SR2 with 1 LSTM layer, batch size of 1 and 100 LSTM cells in each layer.

Figure 7, shows the results of the best model, schematizing the behavior developed by the MSE in the training and testing phases. Superposition of the lines representing each phase represents the efficiency of the model with a proximity greater than 99%. Linear regression developed in the test set represents that the intelligent system has a degree of error lower than 1%, which allows establishing that this intelligent model developed from the implementation of LSTM for the identification of severe slugging flow types is reliable.

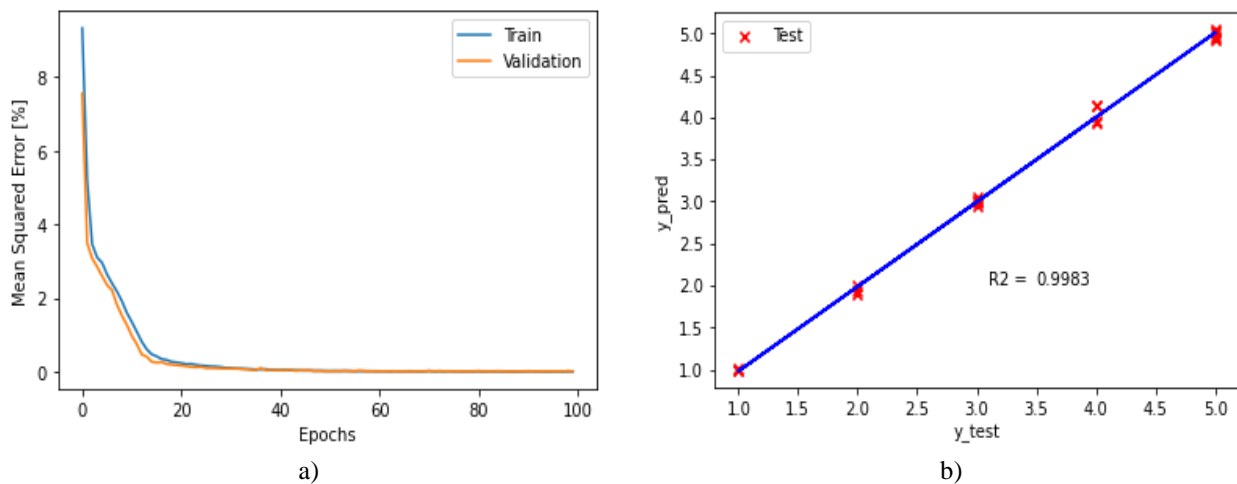


Figure 7. Best model developed: a) Development phases performance b) Linear regression.

Model that developed an efficiency close to the one described above was the one structured with SR1, batch size of 4 and 100 cells in the two LSTM layers that were implemented, reaching an MSE of 0.00367, RMSE of 0.0605 and determining an R² of 0.9982.

6. CONCLUSION

Flow pattern identification in the oil and gas industry is a topic that demands research. In this work a practical methodology based on artificial intelligence is implemented for the development of predictive models, structured with long and short memory networks LSTM, to identify the different types of severe slugging that develop inside the vertical risers present in the industry. We propose an intelligent model whose inputs are the specific density of the gas-liquid mixture (ρ_s), gas-liquid ratio (GLR), superficial gas velocity (USG0), superficial liquid velocity (USL), gas volumetric

fraction (α_G) and liquid volumetric fraction (α_L) and whose output includes the severe slugging types SS1, SS2, SS3, USO and STB. This model presents an MSE of 0.33 % and R^2 of 0.9983, applying SR2 with 1 LSTM layer, batch size of 1 and 100 LSTM cells in each layer.

Additionally, it is proposed as future work the implementation of a LSTM model capable of identifying the types of severe slugging formed with the combination of lubricating oil and Sulfur hexafluoride (SF₆) in vertical piping, whose experimental phase is being developed in the experimental apparatus of the Industrial Multiphase Flows Laboratory of EESC/USP.

7. REFERENCES

- Alhashem, M. (2019, November 11). Supervised Machine Learning in Predicting Multiphase Flow Regimes in Horizontal Pipes. *Day 2 Tue, November 12, 2019*. <https://doi.org/10.2118/197545-MS>
- Alkhalaf, A., Isichei, O., Ansari, N., & Milad, R. (2019). Utilizing Machine Learning for a Data Driven Approach to Flow Rate Prediction. *Day 1 Mon, November 11, 2019*, 1–9. <https://doi.org/10.2118/197266-MS>
- Baliño, J. L., Burr, K. P., & Nemoto, R. H. (2010). Modeling and simulation of severe slugging in air–water pipeline–riser systems. *International Journal of Multiphase Flow*, 36(8), 643–660. <https://doi.org/10.1016/j.ijmultiphaseflow.2010.04.003>
- Goda, H., Kim, S., Mi, Y., Finch, J. P., Ishii, M., & Uhle, J. (2002). Flow Regime Identification of Co-Current Downward Two-Phase Flow With Neural Network Approach. *10th International Conference on Nuclear Engineering, Volume 3*, 71–78. <https://doi.org/10.1115/ICONE10-22088>
- Hasan, A. R., & Kabir, C. S. (1986). A Study of Multiphase Flow Behavior in Vertical Oil Wells: Part I - Theoretical Treatment. *SPE California Regional Meeting, May*, 463–478. <https://doi.org/10.2118/15138-MS>
- Kagemoto, H. (2020). Forecasting a water-surface wave train with artificial intelligence- A case study. *Ocean Engineering*, 207(December 2019), 107380. <https://doi.org/10.1016/j.oceaneng.2020.107380>
- Luo, X., He, L., Liu, X., & Lü, Y. (2014). Influence of separator control on the characteristics of severe slugging flow. *Petroleum Science*, 11(2), 300–307. <https://doi.org/10.1007/s12182-014-0344-3>
- Malekzadeh, R., Henkes, R. A. W. M., & Mudde, R. F. (2012). Severe slugging in a long pipeline-riser system: Experiments and predictions. *International Journal of Multiphase Flow*, 46, 9–21. <https://doi.org/10.1016/j.ijmultiphaseflow.2012.06.004>
- Mi, Y., Ishii, M., & Tsoukalas, L. H. (2001). Flow regime identification methodology with neural networks and two-phase flow models. *Nuclear Engineering and Design*, 204(1–3), 87–100. [https://doi.org/10.1016/S0029-5493\(00\)00325-3](https://doi.org/10.1016/S0029-5493(00)00325-3)
- Park, K. H., Kim, J., Jang, W., & Seo, Y. (2018). Investigation of severe slugging characteristics under various gas-liquid ratio in two-phase flowloop. *Proceedings of the International Offshore and Polar Engineering Conference, 2018-June*, 114–119.
- Pots, B. F. M., Bromilow, I. G., & Konijn, M. J. W. F. (1987). Severe Slug Flow in Offshore Flowline/Riser Systems. *SPE Production Engineering*, 2(04), 319–324. <https://doi.org/10.2118/13723-PA>
- Quintino, A. M., da Rocha, D. L. L. N., Fonseca Jr., R., & Rodriguez, O. M. H. (2020). Flow Pattern Transition in Pipes Using Data-Driven and Physics-Informed Machine Learning. *Journal of Fluids Engineering*, 143(3), 1–11. <https://doi.org/10.1115/1.4048876>
- Ruiz-Diaz, C. M., Gómez-Camperos, J. A., & Hernández-Cely, M. M. (2022). Flow pattern identification of liquid-liquid (oil and water) in vertical pipelines using machine learning techniques. *Journal of Physics: Conference Series*, 2163(1), 012001. <https://doi.org/10.1088/1742-6596/2163/1/012001>
- Schmidt, Z., Brill, J. P., & Beggs, H. D. (1980). Experimental Study of Severe Slugging in a Two-Phase-Flow Pipeline - Riser Pipe System. *Society of Petroleum Engineers Journal*, 20(05), 407–414. <https://doi.org/10.2118/8306-PA>
- Taitel, Yehuda, Barnea, D., & Dukler, A. E. (1980). Modelling flow pattern transitions for steady upward gas-liquid flow in vertical tubes. *AIChE Journal*, 26(3), 345–354. <https://doi.org/10.1002/aic.690260304>
- Taitel, Yehudah, Lee, N., & Dukler, A. E. (1978). Transient gas-liquid flow in horizontal pipes: Modeling the flow pattern transitions. *AIChE Journal*, 24(5), 920–934. <https://doi.org/10.1002/aic.690240518>
- Theyab, M., & Theyab, M. A. (2018). Severe Slugging Control: Simulation of Real Case Study. *J Environ Res*, 2(1), 5. www.imedpub.com
- Wu, Q., Zou, S., Zhang, X., Yang, C., Yao, T., & Guo, L. (2022). Forecasting the transition to undesirable gas-liquid

two-phase flow patterns in pipeline-riser system: A method based on fast identification of global flow patterns. *International Journal of Multiphase Flow*, 149(October 2021), 103998. <https://doi.org/10.1016/j.ijmultiphaseflow.2022.103998>

Yocum, B. T. (1973, April). Offshore Riser Slug Flow Avoidance: Mathematical Models for Design and Optimization. *Proceedings of SPE European Meeting*. <https://doi.org/10.2523/4312-MS>

Zhou, H., Guo, L., Yan, H., & Kuang, S. (2018). Investigation and prediction of severe slugging frequency in pipeline-riser systems. *Chemical Engineering Science*, 184, 72–84. <https://doi.org/10.1016/j.ces.2018.03.050>

8. RESPONSIBILITY NOTICE

C. M. Ruiz-Diaz, Marlon M. Hernández-Cely, and O. M. H. Rodriguez are the only responsible for the printed material included in this paper.